JOURNAL OF APPLIED CRYSTALLOGRAPHY

Volume 55 (2022)

Supporting information for article:

Suppression of phase-transition temperature in aluminium indium tungstate and aluminium indium molybdate

La'Nese Lovings, Dominik Dietzel and Cora Lind

This supporting information document contains additional close-up views of PXRD patterns, Rietveld refinement plots, and Tables with selected lattice constants and refinement statistics.

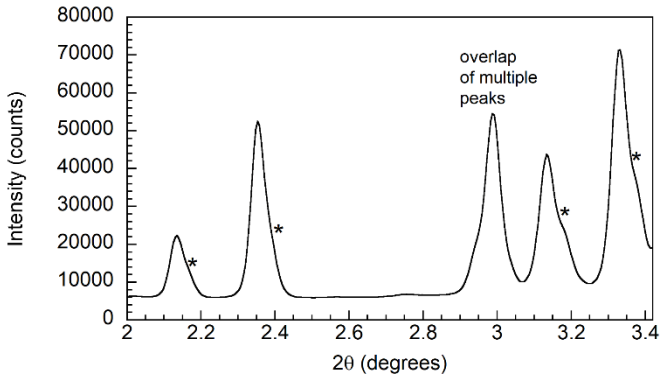

Figure S1 Synchrotron powder diffraction data for $AlInMo_3O_{12}$. Distinct shoulders (*) are observed for all peaks that are dominated by one strong reflection, suggesting the presence of a second phase with a smaller unit cell.

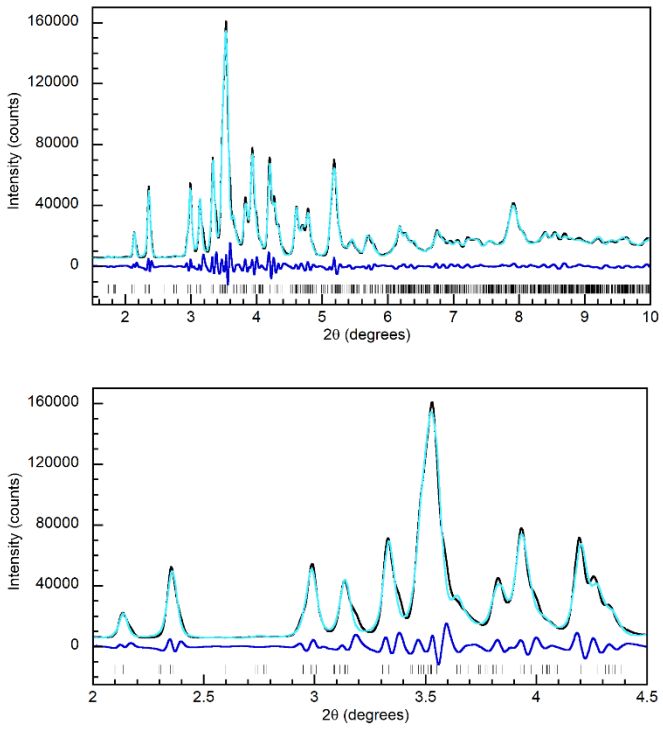

Figure S2 Rietveld plot (full view and zoomed in view of low angle region) using a single monoclinic phase for room temperature synchrotron data collected on the $AlInMo_3O_{12}$ sample. Black: Observed intensity, teal: calculated intensity, blue: difference curve. Tick marks indicate the peak positions of the $A_2M_3O_{12}$ phase. The final refinement statistics were R_{wp} = 6.3% and goodness of fit = 8.4.

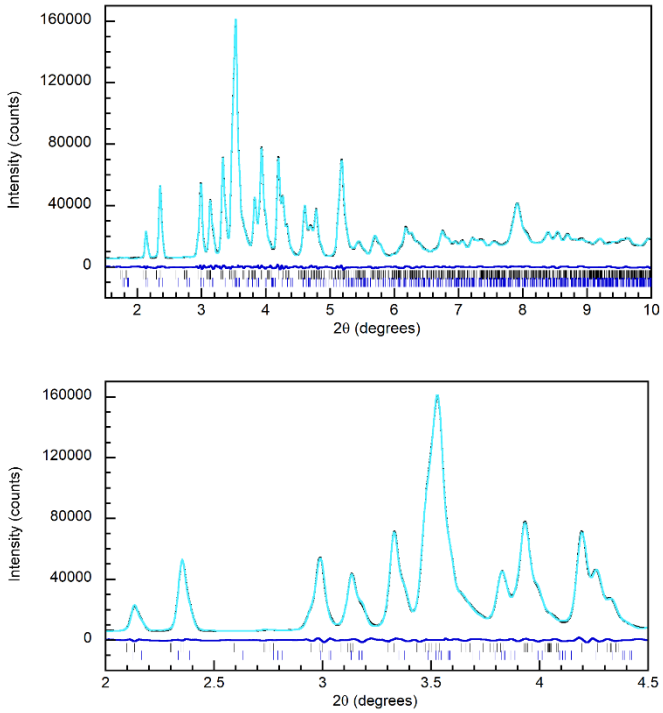

Figure S3 Rietveld plot (full view and zoomed in view of low angle region) using two monoclinic phases for room temperature synchrotron data collected on the $AlInMo_3O_{12}$ sample. Black: Observed intensity, teal: calculated intensity, blue: difference curve. Tick marks indicate the peak positions for the two $A_2M_3O_{12}$ phases. The final refinement statistics were R_{wp} = 1.9% and goodness of fit = 2.4.

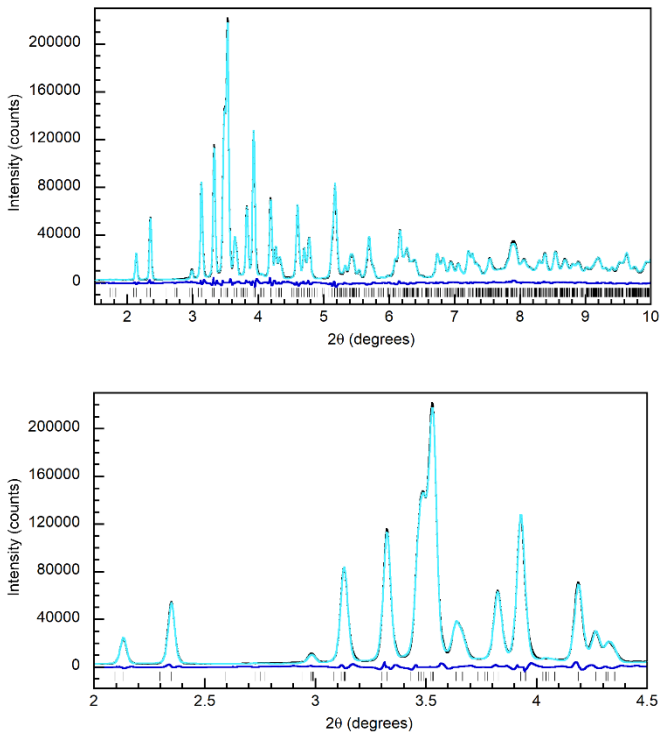

Figure S4 Rietveld plot (full view and zoomed in view of low angle region) using a single monoclinic phase for the 80 K synchrotron data collected on the $AlInW_3O_{12}$ sample. Black: Observed intensity, teal: calculated intensity, blue: difference curve. Tick marks indicate the peak positions of the $A_2M_3O_{12}$ phase. The final refinement statistics were R_{wp} = 3.8% and goodness of fit = 4.6.

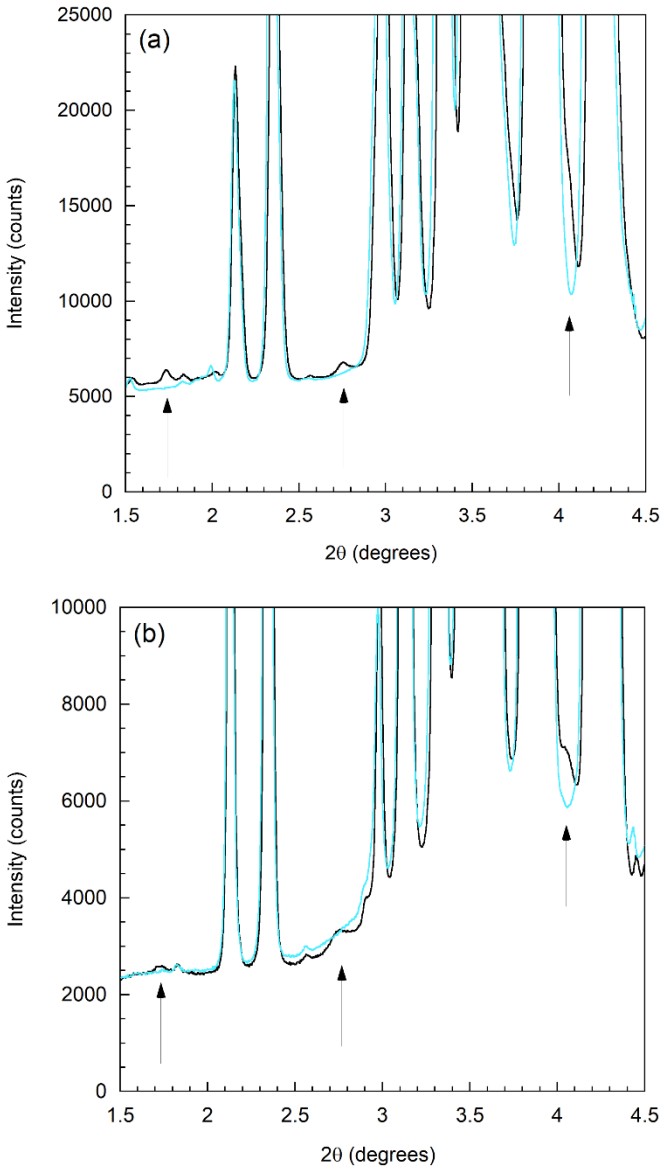

Figure S5 Overlay of synchrotron diffraction patterns collected at the lowest (black) and highest (teal) temperature for (a) $AlInMo_3O_{12}$ and (b) $AlInW_3O_{12}$. Peak positions of distinct monoclinic peaks are marked with arrows.

Table S1 Selected Rietveld refinement results for $Al_{1.16}In_{0/84}Mo_3O_{12}$. For consistency, the minor phase was described with a monoclinic model for all listed refinement results. The monoclinic cell contains twice as many formula units as the orthorhombic cell.

T (K)	R_{wp}	GOF	a (Å)	b (Å)	c (Å)	β (°)	V (Å^3)	B_{iso}
298	1.9	2.4	15.961	9.381	18.513	125.8	2249.3	0.6
323	1.9	2.5	15.966	9.384	18.522	125.8	2251.7	0.7
348	2.0	2.5	15.971	9.389	18.533	125.8	2254.6	0.7
373	2.0	2.7	15.975	9.393	18.545	125.8	2257.8	0.7
398	2.1	2.8	15.980	9.401	18.563	125.8	2262.6	0.8
423	2.1	2.7	15.981	9.407	18.578	125.8	2266.3	0.9
448	2.4	3.2	12.974	9.299	9.413	90	1135.7	1.2
473	2.3	3.0	12.977	9.305	9.417	90	1137.1	1.2
498	2.1	2.8	12.979	9.309	9.421	90	1138.2	1.2
523	2.1	2.7	12.981	9.312	9.423	90	1139.0	1.2
548	2.0	2.6	12.983	9.314	9.424	90	1139.5	1.2
573	2.0	2.6	12.985	9.315	9.425	90	1140.0	1.2
598	2.0	2.6	12.987	9.316	9.425	90	1140.4	1.2
623	2.0	2.6	12.989	9.317	9.426	90	1140.6	1.2
648	2.0	2.6	12.990	9.318	9.426	90	1141.0	1.2
673	2.0	2.6	12.993	9.319	9.426	90	1141.3	1.2
698	2.0	2.6	12.994	9.320	9.427	90	1141.6	1.2
723	2.0	2.6	12.996	9.320	9.427	90	1141.8	1.2

Table S2 Selected Rietveld refinement results for $AlInW_3O_{12}$. The monoclinic cell contains twice as many formula units as the orthorhombic cell.

T (K)	R_{wp}	GOF	a (Å)	b (Å)	c (Å)	β (°)	V (Å^3)	B_{iso}
80	3.8	4.6	15.930	9.385	18.535	125.6	2252.1	1.2
100	3.8	4.6	15.931	9.385	18.537	125.6	2252.5	1.2
125	3.8	4.6	15.932	9.386	18.540	125.6	2253.3	1.2

150	3.9	4.6	15.935	9.388	18.545	125.6	2254.6	1.2
175	3.9	4.6	15.937	9.390	18.550	125.6	2256.0	1.3
200	3.9	4.6	15.941	9.392	18.556	125.6	2257.5	1.3
225	3.8	4.6	15.943	9.394	18.562	125.7	2259.0	1.3
250	3.8	4.6	15.946	9.395	18.567	125.7	2260.3	1.4
275	4.2	5.0	12.959	9.286	9.397	90	1130.9	1.9
300	4.1	4.8	12.961	9.289	9.398	90	1131.5	1.9
325	4.0	4.7	12.963	9.290	9.399	90	1132.0	1.9
350	3.9	4.6	12.965	9.292	9.400	90	1132.4	2.0
375	3.9	4.6	12.967	9.293	9.401	90	1132.9	2.0
400	3.9	4.6	12.969	9.295	9.401	90	1133.2	2.0
425	3.8	4.5	12.971	9.296	9.402	90	1133.6	2.0
450	3.8	4.5	12.973	9.297	9.402	90	1134.0	2.1
475	3.8	4.5	12.975	9.298	9.403	90	1134.3	2.1
500	3.9	4.6	12.977	9.298	9.403	90	1134.6	2.1